Macromolecules

pubs.acs.org/Macromolecules Article

Controlling Dynamics of Associative Networks through Primary Chain Length

Jacob J. Lessard,[‡] Kevin A. Stewart,[‡] and Brent S. Sumerlin*

Cite This: *Macromolecules* 2022, 55, 10052−10061 Read Online

ACCESS | Metrics & More | Article Recommendations | Supporting Information

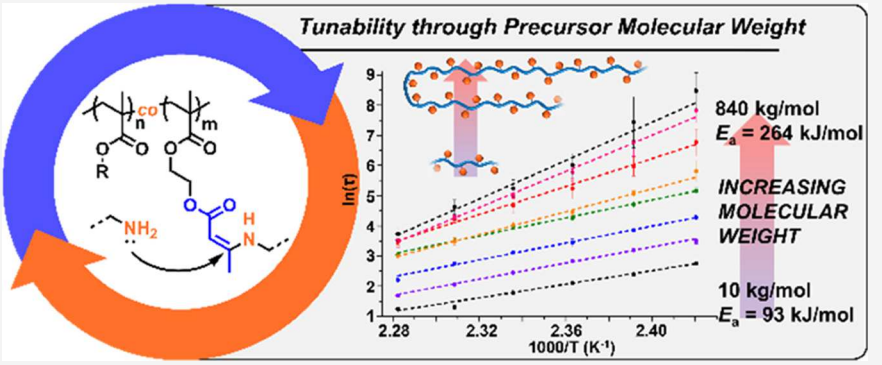

ABSTRACT: Dynamic networks couple the robust nature of thermosets with the shapeability and recyclability of thermoplastics. Though a wealth of exchange chemistries can be leveraged to fabricate dynamic networks, reversibly cross-linked systems that are comprised primarily of chains with nonexchangeable backbones increase the network complexity and render flow behavior difficult to predict. Here, we report the flow behavior of polymethacrylate-based vitrimers prepared by cross-linking β-ketoester-containing polymers with multifunctional amines and demonstrate that the molecular weight and dispersity of the primary chains can be tuned to actively tailor the dynamics of the resulting networks. Vitrimers of similar composition and cross-link density made from polymers below and well above the entanglement molecular weight exhibited distinct viscoelastic flow properties with energies of activation ranging from 93 to 264 kJ/mol. Resistance to creep increased dramatically with increasing primary chain length. Finally, blending of prepolymers to skew M_n above/below M_e was demonstrated, showing a distinguishable effect of prepolymer breadth and skewness on vitrimer flow. Our results suggest that tailoring the molecular weight and chain-length distribution of the primary chain polymers is a viable strategy to design materials with predictable viscoelastic properties and customizable vitrimer flow behavior.

INTRODUCTION

The increase in the global production of commodity plastics has accelerated the development of efficient recycling strategies.[1,2] Current recycling efforts are directed primarily to thermoplastics, i.e., materials comprised of discreet polymer chains, which can be easily molded and readily recycled through heat or solvent exposure. However, thermoplastics often have reduced mechanical, thermal, and chemical durability compared to their cross-linked thermoset counterparts. Thermosets are composed of polymer chains that are largely immobilized due to their cross-linked nature. While this feature precludes their recyclability and reprocessability, thermosets maintain their robust properties even at elevated temperatures or solvent exposure. Innovative approaches have been developed to enable cross-link reversibility to access materials that maintain their network structure while providing avenues for reprocessability.[3−13]

Covalent adaptable networks (CANs) are cross-linked polymers where the covalent connectivity between chains is reversible and allows network rearrangement upon exposure to various stimuli—most commonly the application of heat. Design strategies employing stimuli-responsive network rearrangement have led to robust materials that are moldable, reprocessable, self-healing, and recyclable.[6−8] CANs come in two forms, depending on the nature of their bond exchange mechanism (Figure 1). Dissociative CANs rely on the equilibrium of bond breakage and reformation to facilitate polymer flow. Complete network (bond) reformation is possible upon removal of the requisite stimulus. This equilibrium-driven process lends dissociative CANs a level of variability in the overall network integrity following reprocessing.[14−16] Associative CANs are networks that bear functional

Received: September 15, 2022
Revised: October 17, 2022
Published: November 2, 2022

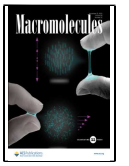

https://doi.org/10.1021/acs.macromol.2c01909
Macromolecules 2022, 55, 10052−10061

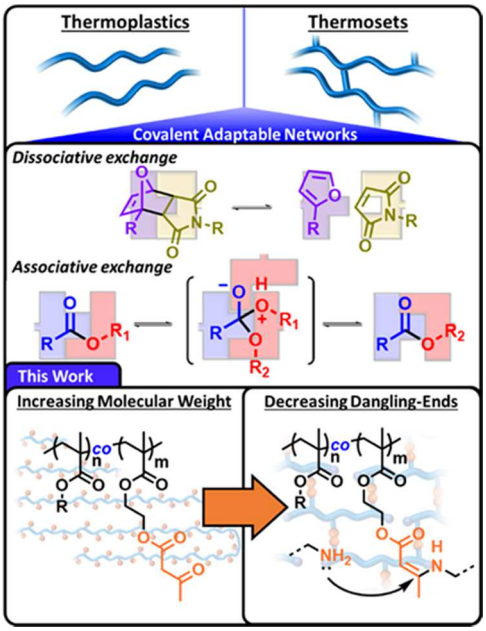

Figure 1. (Top) Illustration of the structural differences between thermoplastics and thermosets. (Middle) Examples of dissociative and associative exchange chemistries used to furnish CANs. (Bottom) Targeting incrementally higher degrees of polymerization for vitrimer prepolymers leading to increased physical entanglements/decreased dangling ends.

groups capable of reacting with existing cross-links to form a new cross-link while simultaneously liberating an identical reactive moiety. Because one cross-link is exchanged for another, this degenerative process allows for network rearrangement with the conservation of cross-link density, which safeguards network integrity. The unique flow capability of dissociative and associative CANs overcomes the lack of processability and recyclability of traditional thermoset materials.[17,18]

While some of the first reports of elastomers with exchangeable cross-links date to at least the 1950s, Bowman and co-workers championed the concept of associative CANs in 2005−2009.[19−22] Subsequent seminal reports by Leibler and co-workers introduced the term "vitrimers" to describe materials with Arrhenius-like viscosity dependence analogous to vitreous silica.[23,24] In the decade since, research concerning these dynamically cross-linked materials has evolved at a rapid pace. Increased understanding of the fundamentals that govern vitrimer rheology over this relatively short timeframe has resulted in a host of strategies to control or predict flow behavior.[25−28] Research has largely focused on three synthetic approaches to tune the rheological properties of vitrimers: modifying or compounding the exchange chemistry at the cross-link site(s),[29−46] introduction of internal or external catalysts (or inhibitors),[47−57] and varying the matrix composition, polarity, and architecture.[17,58−68]

Our group has employed controlled radical polymerization as a tool to facilitate the study of structure−property relationships between polymer properties and vitrimer flow. Specifically, reversible addition-fragmentation chain-transfer (RAFT) polymerization was used to prepare both statistical and block methacrylate copolymers of controlled molecular weight for enaminone vitrimer formation.[18,66,67] The versatility afforded by this living polymerization approach led us to consider whether it is possible to preordain viscoelastic flow behavior by targeting specific molecular weights of prepolymers that can be subsequently cross-linked to form associative networks. We reasoned that this strategy may provide important new design principles to tailor networks with predictable reprocessability and viscoelastic properties without changing cross-link chemistry, cross-link density, or network composition. Accordingly, we hypothesized that increasing the molecular weight of the polymer backbone would reduce network mobility and hamper the viscoelastic flow in the resulting vitrimer. In this report, we employed RAFT polymerization to synthesize polymers of butyl methacrylate (BMA) and 2-acetoacetoxyethyl methacrylate (AAEMA) with predetermined molecular weights. The resulting copolymers (P(BMA-*co*-AAEMA)) were cross-linked with a multifunctional amine at identical ratios of cross-linker to free amines, ensuring a uniform cross-link density and amine content across the molecular weight range. We expected that the molecular weight of the pre-cross-linked polymers would play an important role in dictating flow behavior and provide a new parameter for the precision design of vitrimers for specific processing conditions and applications.

RESULTS AND DISCUSSION

Polymer Synthesis and Characterization. To evaluate the feasibility of specifically exploiting differences in primary chain length to tune viscoelastic properties, it was first necessary to synthesize cross-linkable polymers of varying molecular weights. Accordingly, statistical copolymers of BMA and AAEMA (1:1 molar ratio) were prepared by RAFT polymerization,[69,70] a well-suited platform for the synthesis of vinyl-derived vitrimer systems (Figure 2).[18,67,71] By varying the chain-transfer agent to monomer ratio, polymers with a number-average molecular weight (M_n) of 10, 20, 30, 50, 70, 90, 280, and 840 kg/mol were synthesized with dispersity values ranging from 1.2 to 1.6 (Figure 2A). After polymer synthesis, RAFT-generated thiocarbonylthio end groups were removed for polymers under 280 kg/mol to reduce the contribution of potential side reactions during cross-linking (Figure 2, Table S1, and Figures S1−S18). NMR spectroscopic characterization indicated that all eight P(BMA-*co*-AAEMA) samples contained similar AAEMA incorporations ranging from 49 to 52% across the molecular weight range (Figure 2B).

To understand the role of chain entanglement in the flow behavior of the final vitrimers, we first determined the entanglement molecular weight (M_e) for the copolymers prior to cross-linking (Figure 2C,D). M_e can be determined through frequency sweep experiments of polymers of molecular weight assumed to be well above M_e. Extrapolating the plateau modulus (G_n)—the storage modulus (G') at the minimum tan(δ)—the M_e can be calculated based on eq S1.[72] Polymers below the M_e should lack a crossover point in the frequency sweep that is characteristic of the material transitioning from a viscoelastic solid ($G'' < G'$) to a viscoelastic fluid ($G'' > G'$), i.e., the loss modulus (G'') should remain above storage modulus (G') after the glass transition.

The prepolymers were compression-molded at 60 °C into disks for shear rheology, and frequency sweeps were performed at varying temperatures for each polymer. A crossover for G' and G'' was observed for polymers of 50 kg/mol and above (Figure 2C, Tables S1 and S2, and Figures S19−S29), allowing an M_e of 26 kg/mol to be calculated from the prepolymer with M_n = 50 kg/mol. For polymers of higher molecular weights

https://doi.org/10.1021/acs.macromol.2c01909
Macromolecules 2022, 55, 10052−10061

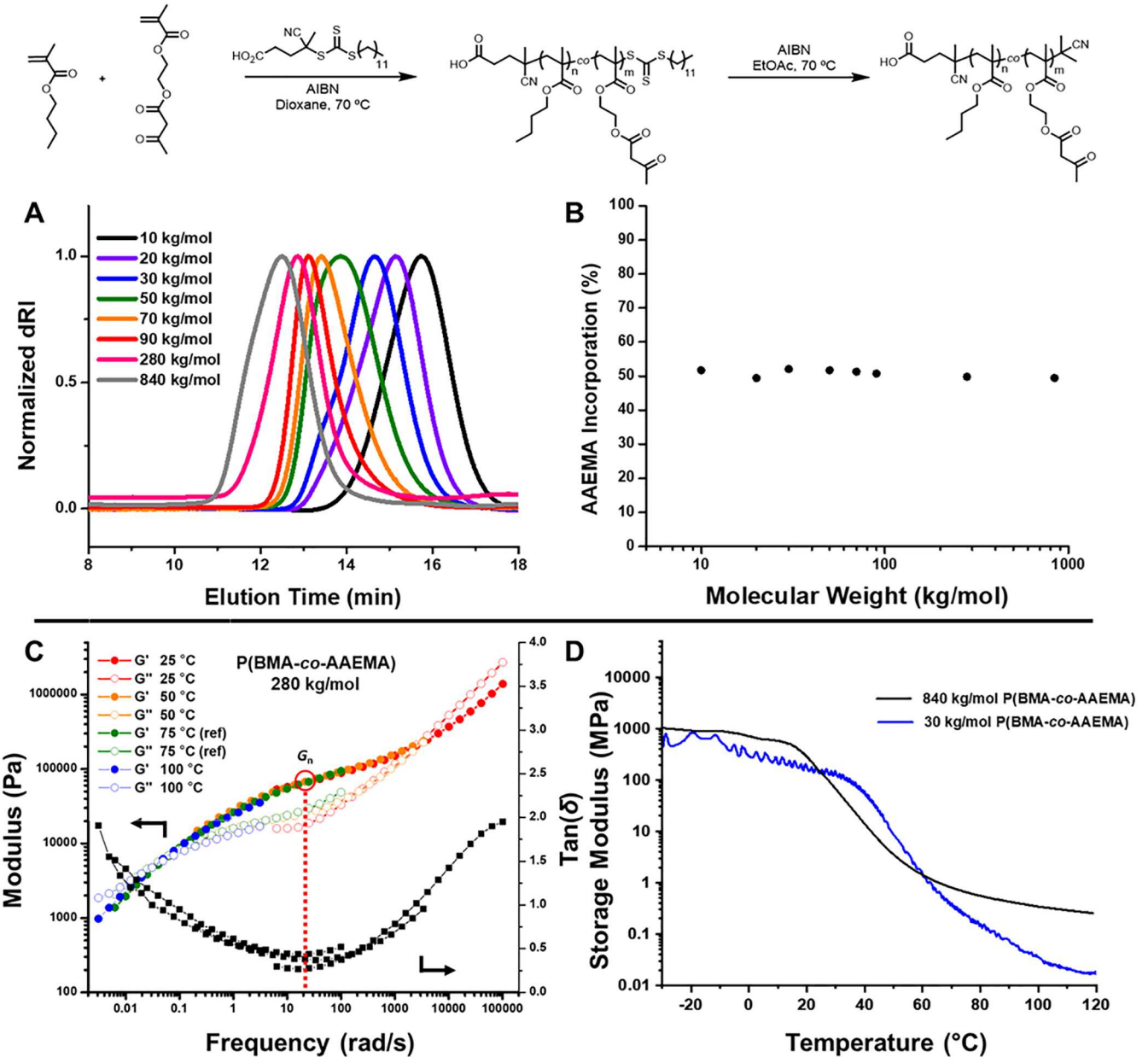

Figure 2. (A) GPC traces of P(BMA-*co*-AAEMA) of varying molecular weights. (B) AAEMA incorporation of P(BMA-*co*-AAEMA) at varying molecular weights. (C) Master plot from frequency sweeps at a 0.3% oscillating strain at 25, 50, 75, and 100 °C for 280 kg/mol P(BMA-*co*-AAEMA), showing the storage modulus (G'), loss modulus (G''), and tan(δ) using time−temp superposition (75 °C ref). (D) Oscillatory tensile temperature sweep from dynamic mechanical analysis for 840 kg/mol (black) and 30 kg/mol (blue) P(BMA-*co*-AAEMA).

(70, 100, 280, and 840 kg/mol), the M_e plateaued at 38 ± 3 kg/mol. The calculated M_e from the polymers above 70 kg/mol agrees well with the absence of a crossover in the frequency sweeps for polymers of 30 kg/mol and lower (Table S3). Additionally, we used dynamic mechanical analysis (DMA) to determine the rubbery plateau modulus from a temperature sweep of prepolymer M_n = 840 kg/mol (eq S2) to calculate an M_e of 26 kg/mol (Figure 2D, black). This value aligns well with the lack of an observed rubbery plateau in the DMA thermogram for the 30 kg/mol prepolymer (Figure 2D, blue).

Vitrimer Synthesis and Characterization. P(BMA-*co*-AAEMA)-derived vitrimers were prepared by solution casting the prepolymers from tetrahydrofuran (THF) with 0.9 equiv of xylylene diamine to AAEMA monomer units. After curing, the resulting vitrimers were broken into shards and compression-molded at 160 °C under vacuum to yield geometries that permitted characterization by Fourier transform infrared (FTIR) spectroscopy, differential scanning calorimetry (DSC), DMA, and rheological studies (Figures 3A and S30). FTIR spectroscopy of all vitrimers displayed characteristic signals of enaminones at ∼1600 and ∼1650 cm^{-1} corresponding to C═C stretching and N−H bending, respectively (Figures S31 and S32). The glass-transition temperature (T_g) of the resulting vitrimers was relatively consistent over the range of 53−76 °C, as determined by DSC (Table S4). Finally, the network structure of the vitrimers was verified by the rubbery plateau observed in all DMA thermograms (eq S2, Figure S33, and Table S5).

https://doi.org/10.1021/acs.macromol.2c01909
Macromolecules 2022, 55, 10052−10061

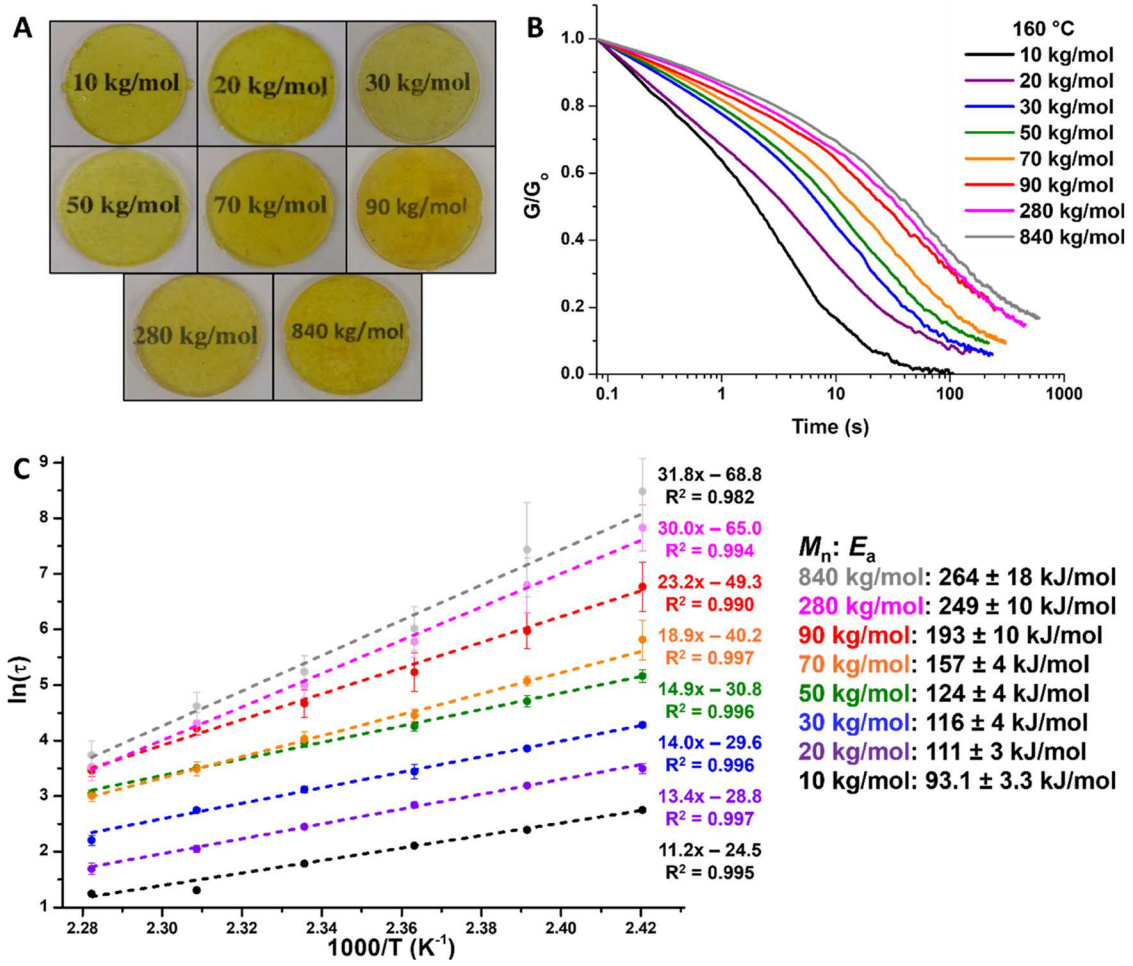

Figure 3. (A) Images of vitrimers after compression molding. (B) Normalized stress relaxation (0.3% strain) of vitrimers of varying prepolymer molecular weights at 160 °C. (C) Arrhenius plots and activation energy of viscous flow (E_a) from stress relaxation data for vitrimers with varying prepolymer molecular weights (τ at $G/G_0 = 1/e$, 5 °C increments from 165 to 140 °C).

The relaxation of force (stress) from an instantaneous deformation (strain, 0.3%) showed a clear reliance on the molecular weight of the prepolymer within the vitrimer network (Figures 3B and S34−S41). The rate of relaxation for the vitrimers decreased as molecular weight increased, a trend also observed in uncross-linked, linear polymers.[73] The stress relaxation times for the different vitrimers were fitted to the Arrhenius equation, where the characteristic relaxation time (τ, i.e., the inverse rate constant for viscoelastic flow assuming a Maxwell model) was taken as the time when $G/G_o = 1/e$ and was plotted against inverse temperature (Figure 3C). The resulting slope of the Arrhenius plot yielded the activation energy for viscous flow (E_a) of the material.

The vitrimers synthesized from prepolymers of $M_n \leq M_e$ (10, 20, and 30 kg/mol) had E_a values of 93.1 ± 3.3, 111 ± 3, and 116 ± 4 kJ/mol, respectively, which agree well with the E_a values determined for vitrimers in previous reports.[18,67] Interestingly, vitrimers made from prepolymers of $M_n > M_e$ (50, 70, and 90 kg/mol) had activation energies that followed a more considerable increasing trend from 124 ± 4, 157 ± 4, and 193 ± 10 kJ/mol; however, the E_a for vitrimers made from prepolymers with M_n > 90 kg/mol began to plateau in the range of 250−264 kJ/mol (Figures 4A and S42). The increase in E_a and the decrease in the relaxation rate of the vitrimers of increasing prepolymer molecular weight suggest that the average size of the prepolymer contributes significantly to the flow behavior of the material. The apparent plateau of τ with increasing prepolymer M_n suggests a critical threshold of physical entanglements above which viscous flow is heavily impeded (Figure 4B, blue).

We further investigated the viscoelastic flow behavior of the vitrimers through frequency sweeps and creep-recovery experiments at 150 °C (Figures 4B and S43−S50). The frequency sweeps displayed a similar trend as that shown in the stress relaxation tests exhibiting decreased flow of the vitrimers with increasing prepolymer molecular weight, as indicated by the lower frequencies for the crossovers of G' and G'' as the viscoelastic fluid ($G'' > G'$) transitions to viscoelastic solid ($G'' < G'$). Again, the vitrimers of highest prepolymer molecular weights (100, 280, and 840 kg/mol) showed plateauing of the inverse crossover points (Figure 4B, red), implying a relatively constant recovery flow rate at high molecular weights, a trend similar to that observed with the characteristic relaxation time in stress relaxation experiments. Creep-recovery experiments were used to calculate the zero-shear viscosity (η_o) of the materials. Again, the η_o increased in a similar fashion to both the crossover from frequency sweeps and the characteristic relaxation from stress relaxation experiments, plateauing at higher prepolymer molecular weights (Figure 4B, black). The maximum strain percentage, i.e., how far the material deforms upon an applied stress, generally decreased as molecular weight increased. Vitrimers of prepolymer M_n below 50 kg/mol

https://doi.org/10.1021/acs.macromol.2c01909
Macromolecules 2022, 55, 10052−10061

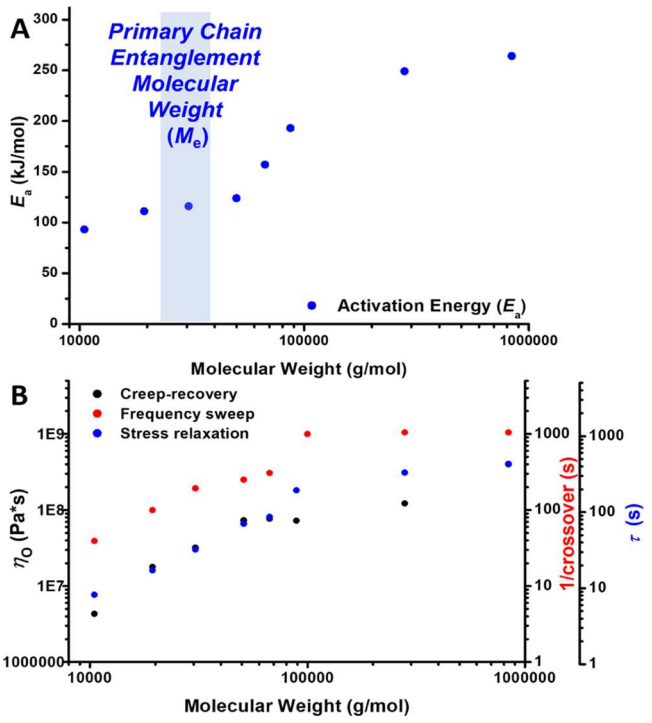

Figure 4. (A) Plot of the activation energy of viscous flow (E_a) vs molecular weight, showing a dramatic increase in E_a for vitrimers prepared from prepolymers with M_n values that ranged from below to well above the entanglement molecular weight (M_e). (B) Zero-shear viscosity from creep experiments (black), inverse crossover times from frequency sweeps (red), and τ from stress relaxation tests (blue) for vitrimers at 150 °C vs the number-average molecular weight of prepolymers. These results indicate that flow behavior is impeded as molecular weight increases, though the effect begins to plateau well above M_e.

displayed elevated levels of creep, with the 10 kg/mol sample being the most affected (Figure S50). Vitrimers prepared from prepolymers of M_n of 50, 70, and 90 kg/mol displayed less creep, and their maximum strain percentages were within 1% of one another. Finally, for the vitrimers of prepolymers M_n = 280 and 840 kg/mol, the trend was further highlighted, reaching only 2.90 and 0.58% strain, respectively. Thus, increasing the primary chain molecular weight imparts a strong resistance to deformation at elevated temperatures. Moreover, the percent recovery from creep experiments generally increased with molecular weight. Specifically, for vitrimers from prepolymers of M_n = 10−90 kg/mol, the recovery percentages of the vitrimers steadily increased; however, for vitrimers from prepolymer M_n = 280 and 840 kg/mol, the trend appeared to reverse, resulting in lower percent recoveries. However, the dramatic decrease in strain percentages in vitrimers from prepolymers with $M_n > M_e$ indicates enhanced elastic behavior as a function of molecular weight. Clearly, the elastic character of the vitrimers dominates as molecular weight increases, attributable to the increasing levels of physical entanglements, which impede the productive bond exchange and, thus, viscous flow. These data consistently show that vitrimer primary chain length has a remarkable effect on flow behavior in terms of temperature sensitivity, rate of flow, and resistance to deformation.

After confirming that control over prepolymer size can be exploited to tailor the flow behavior of vitrimers, we also wanted to understand the influence of molecular weight distribution on vitrimer processing. Classically, polymer distributions have been described as the ratio of the weight-average molecular weight, M_w, to M_n, denoted as $Đ$. However, recently, there has been an increased appreciation that $Đ$ does not thoroughly express chain-length distributions, indicating a significant contribution of distribution shape and breadth.[74−77] With this in mind, we blended prepolymers to skew the molecular weight distributions to higher and lower molecular weights while maintaining a relatively consistent M_n. By mixing a majority (by weight) of 70 kg/mol prepolymer with the 10 kg/mol prepolymer, a sample with M_n of 30 kg/mol was isolated to represent a polymer with a distribution skewed to the higher end of molecular weights as a counterpart for the previously studied 30 kg/mol prepolymer (Figure 5A).

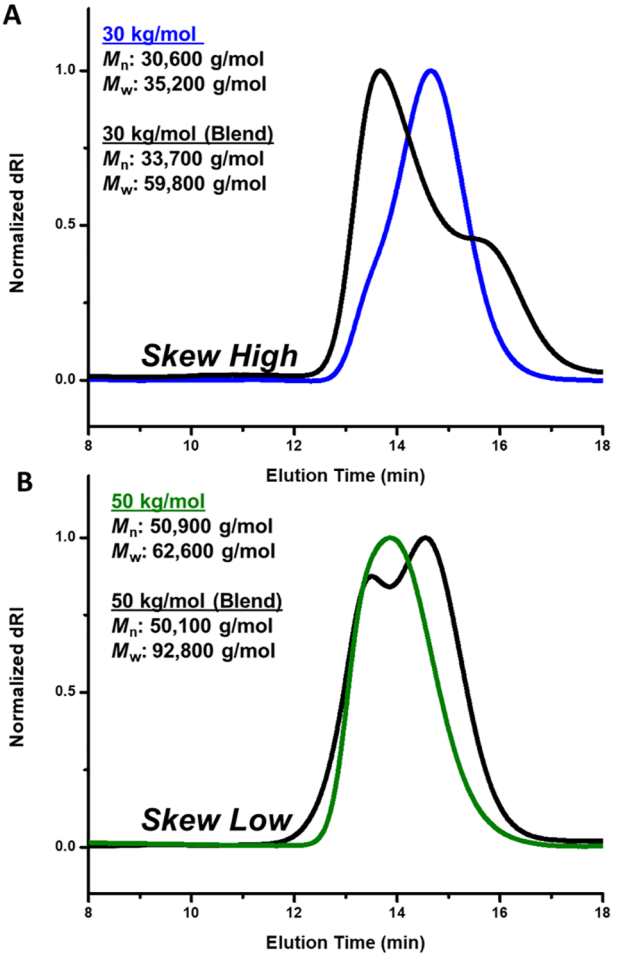

Figure 5. (A) Overlayed GPC chromatograms of skewed-high 30 kg/mol and 30 kg/mol prepolymers. (B) Overlayed GPC chromatograms of skewed-low 50 kg/mol and 50 kg/mol prepolymers.

Similarly, 90 kg/mol (minor) and 30 kg/mol (major) prepolymers were blended to form a polymer with an M_n of 50 kg/mol and a distribution that was skewed to the lower end of the molecular weight distribution as a counterpart to the nonskewed 50 kg/mol prepolymer (Figures 5B and S51). The resulting polymers were cross-linked, and vitrimer characterization experiments were conducted (Figures S52−S54).

In creep-recovery experiments, the skewed-high 30 kg/mol vitrimer reached approximately the same strain percentage as the nonskewed 30 kg/mol counterpart (8.25 and 8.52%,

https://doi.org/10.1021/acs.macromol.2c01909
Macromolecules 2022, 55, 10052−10061

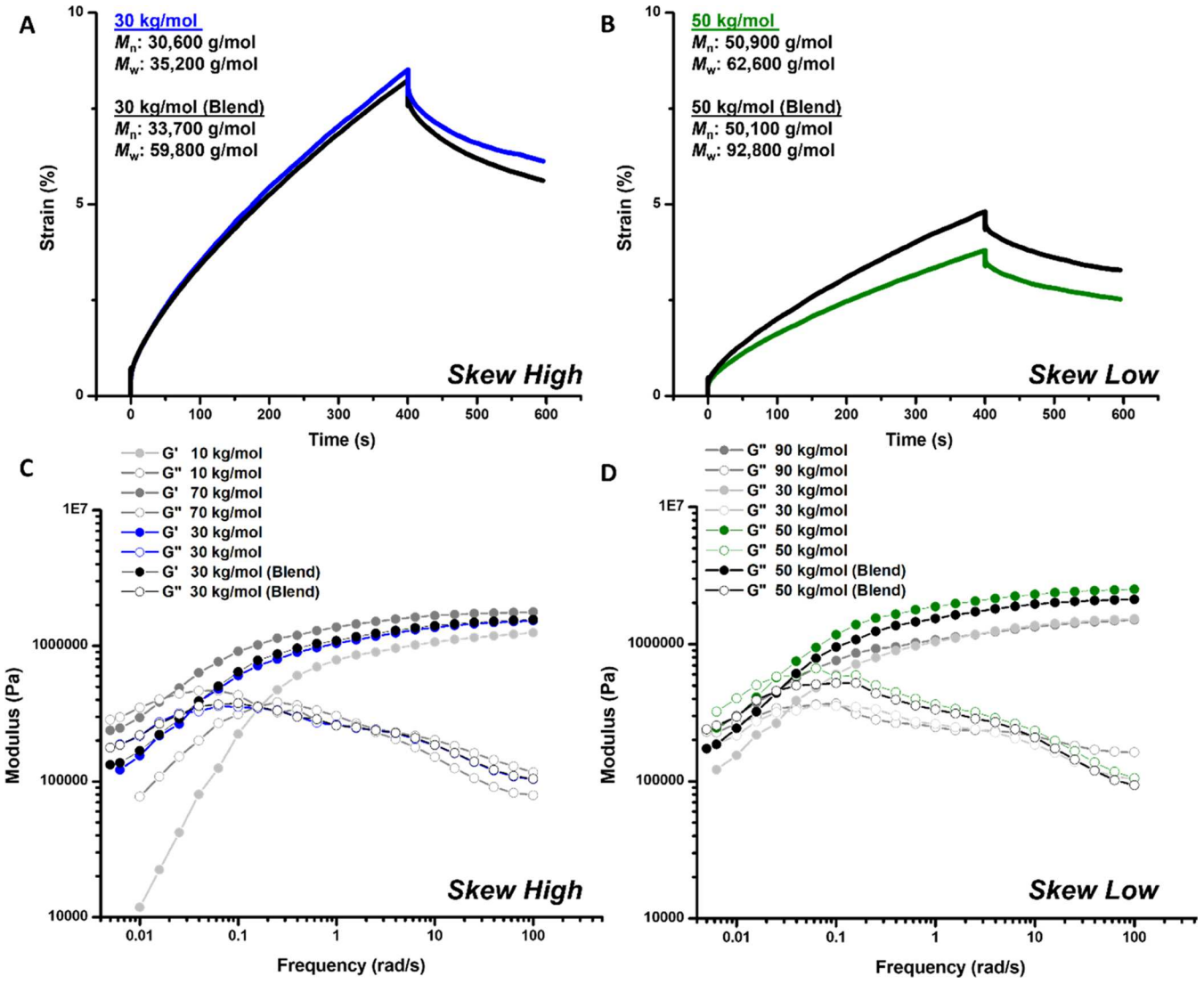

Figure 6. (A) Overlayed creep-recovery curves of vitrimers prepared from skewed-high 30 kg/mol (black) and the nonskewed 30 kg/mol (blue) prepolymers showing increased elastic recovery with a skewed-high size distribution. (B) Overlayed creep-recovery curves of vitrimers prepared from skewed-low 50 kg/mol (black) and the nonskewed 50 kg/mol (green) prepolymers showing increased permanent deformation from enhanced viscous flow with a skewed-low size distribution. (C) Frequency sweeps at a 0.3% oscillating strain of vitrimers prepared from skewed-high 30 kg/mol (black) and the nonskewed 30 kg/mol (blue), overlayed with the 70 kg/mol (dark gray) and 10 kg/mol vitrimers (light gray) used to prepare skewed-high vitrimer. (D) Frequency sweeps at a 0.3% oscillating strain of skewed-low 50 kg/mol vitrimer (black) and the nonskewed 50 kg/mol vitrimer (green), overlayed with the 90 kg/mol (dark gray) and the 30 kg/mol vitrimers (light gray) used to prepare skewed-low vitrimer.

respectively); however, the percent recovery increased for the skewed system (31.8 and 28.1%, respectively), implying that the contribution of higher-molecular-weight chains led to an increase in elastic behavior via increased physical entanglements (Figure 6A). This is further supported by the strain percentage observed for the vitrimer prepared from the skewed-low 50 kg/mol prepolymer (Figure 6B), as the maximum strain was higher than its nonskewed counterpart (4.81 and 3.80%, respectively), with both having similar percent recoveries (31.8 and 33.7%, respectively). Interestingly, frequency sweeps at 150 °C revealed that the skewed polymer samples possessed nearly identical crossover points of G' and G'' as their counterparts (Figure 6C,D).

Stress relaxation tests of the skewed-high 30 kg/mol vitrimer displayed a decreased flow rate and an increased E_a compared to the vitrimer prepared from the nonskewed 30 kg/mol prepolymer (Figures 7A and S53). This result suggests that the presence of the high-molecular-weight component limits the flow rate of the vitrimer, with the chains above M_e increasing the energy barrier for flow. Such findings may indicate that when the majority of the prepolymer population is above M_e, a "sticky reptation" model of polymer flow is adopted, and polymer diffusion dominates cross-link exchange to limit viscous flow.[78−82] Furthermore, increased entanglements may result in spatially trapped cross-links, restricting viscous flow.[83] Interestingly, when the molecular weight distribution was skewed low, the rate of relaxation was faster at high temperatures, and the vitrimer was much more sensitive to changes in temperature (i.e., higher E_a).

This result suggests that the higher end of the molecular weight distribution is dictating the energy barrier needed for flow, while the increased relaxation rate at high temperatures

https://doi.org/10.1021/acs.macromol.2c01909
Macromolecules 2022, 55, 10052−10061

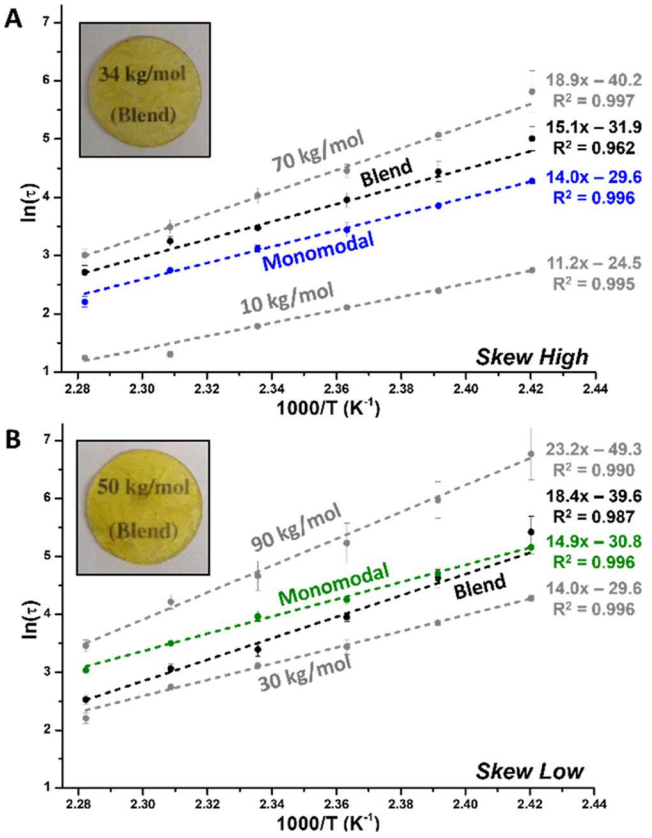

Figure 7. (A) Arrhenius relationship of vitrimers from stress relaxation at 0.3% strain (τ at $G/G_0 = 1/e$, 5 °C increments from 165 to 140 °C, performed in triplicate) comparing monomodal (blue), skewed-high molecular weight (black), and vitrimers from prepolymers used to prepare the skewed-high vitrimer (gray). The inset image of skewed-high vitrimer. (B) Arrhenius relationship of vitrimers from stress relaxation at 0.3% strain (τ at $G/G_0 = 1/e$, 5 °C increments from 165 to 140 °C, performed in triplicate) comparing monomodal (green), skewed-low molecular weight (black), and vitrimers from prepolymers used to prepare the skewed-low vitrimer (gray). The inset image of skewed-low vitrimer.

may be dictated by the overall distribution of the polymer (Figures 7B and S54). Specifically, when the majority of the prepolymer population is below M_e, a "sticky Rouse" model is favored at elevated temperatures, and cross-link exchange is the dominant barrier to viscous flow rather than the diffusion of entangled backbones.[84−88] This explanation agrees well with the creep data for the skewed-low 50 kg/mol-based vitrimer (higher strain % compared to the unskewed counterpart), again indicating that the population of polymers below M_e imparts an increase to the viscous component of the material at higher temperatures through unimpaired polymer diffusion. Primary chains below M_e dilute those that are above M_e, decreasing the secondary network junctions and dampening the viscous flow of the material through chain segmental motion. Thus, it is feasible to tune the reaction-controlled and diffusion-controlled contributions to the flow of vitrimers by both narrowing/broadening and skewing the molecular weight distribution of the prepolymers.

CONCLUSIONS

Active control over vitrimer flow properties and temperature sensitivity is crucial for the translation of vitrimer materials into industrial applications where efficient (re)processing is often defined by thermal requirements. The results presented here demonstrate that carefully selecting the molecular weight of prepolymers prior to associative cross-linking is a viable method to tune the properties of vitrimers without changing the specifics of cross-link chemistry, cross-link density, or network composition. Increasing prepolymer molecular weight leads to increased creep resistance, increased viscous flow E_a, and decreased relaxation and recovery flow rate. Flow studies of vitrimers comprised of prepolymers, with both broadened and skewed molecular weight distributions further demonstrating the influence of prepolymer molecular weight on vitrimer flow behavior by showing that the effects cannot simply be described by prepolymer M_n or M_w but are also affected by the shape of the distribution (i.e., breadth and skewness). Our results suggest that vitrimer melts from prepolymers above and below the molecular weight of entanglement have distinct, diffusion-controlled viscoelastic behavior. This report provides important new design principles for tailoring vitrimers with preordained flow behavior.

ASSOCIATED CONTENT

Supporting Information

The Supporting Information is available free of charge at https://pubs.acs.org/doi/10.1021/acs.macromol.2c01909.

Materials and instrumentation; polymer synthesis and characterization; vitrimer synthesis; rheology; molecular weight skewness; and references (PDF)

AUTHOR INFORMATION

Corresponding Author

Brent S. Sumerlin − *George & Josephine Butler Polymer Research Laboratory, Center for Macromolecular Science & Engineering, Department of Chemistry, University of Florida, Gainesville, Florida 32611, United States;* orcid.org/0000-0001-5749-5444; Email: sumerlin@chem.ufl.edu

Authors

Jacob J. Lessard − *George & Josephine Butler Polymer Research Laboratory, Center for Macromolecular Science & Engineering, Department of Chemistry, University of Florida, Gainesville, Florida 32611, United States;* orcid.org/0000-0003-2962-6472

Kevin A. Stewart − *George & Josephine Butler Polymer Research Laboratory, Center for Macromolecular Science & Engineering, Department of Chemistry, University of Florida, Gainesville, Florida 32611, United States*

Complete contact information is available at: https://pubs.acs.org/10.1021/acs.macromol.2c01909

Author Contributions

‡J.J.L. and K.A.S. contributed equally to this work. The manuscript was written through contributions of all authors. All authors have given approval to the final version of the manuscript.

Notes

The authors declare no competing financial interest.

ACKNOWLEDGMENTS

This material was based upon work supported by the National Science Foundation (NSF DMR-1904631). The authors thank Anton Paar for the use of the Anton Paar 702 rheometer through their VIP academic program. The authors would also

like to thank Dr. Georg M. Scheutz for helpful discussions about this work.

REFERENCES

(1) Millican, J. M.; Agarwal, S. Plastic Pollution: A Material Problem? *Macromolecules* **2021**, *54*, 4455−4469.
(2) Horejs, C. Solutions to Plastic Pollution. *Nat. Rev. Mater.* **2020**, *5*, No. 641.
(3) Hayashi, M. Versatile Functionalization of Polymeric Soft Materials by Implanting Various Types of Dynamic Cross-Links. *Polym. J.* **2021**, *53*, 779−788.
(4) Zou, W.; Dong, J.; Luo, Y.; Zhao, Q.; Xie, T. Dynamic Covalent Polymer Networks: From Old Chemistry to Modern Day Innovations. *Adv. Mater.* **2017**, *29*, No. 1606100.
(5) Van Zee, N. J.; Nicolaÿ, R. Vitrimers: Permanently Crosslinked Polymers with Dynamic Network Topology. *Prog. Polym. Sci.* **2020**, *104*, No. 101233.
(6) Sumerlin, B. S. Next-Generation Self-Healing Materials. *Science* **2018**, *362*, 150−151.
(7) Scheutz, G. M.; Lessard, J. J.; Sims, M. B.; Sumerlin, B. S. Adaptable Crosslinks in Polymeric Materials: Resolving the Intersection of Thermoplastics and Thermosets. *J. Am. Chem. Soc.* **2019**, *141*, 16181−16196.
(8) Kloxin, C. J.; Bowman, C. N. Covalent Adaptable Networks: Smart, Reconfigurable and Responsive Network Systems. *Chem. Soc. Rev.* **2013**, *42*, 7161−7173.
(9) Wang, S.; Urban, M. W. Self-Healing Polymers. *Nat. Rev. Mater.* **2020**, *5*, 562−583.
(10) Taplan, C.; Guerre, M.; Du Prez, F. E. Covalent Adaptable Networks Using β- Amino Esters as Thermally Reversible Building Blocks. *J. Am. Chem. Soc.* **2021**, *143*, 9140−9150.
(11) Wang, S.; Ma, S.; Li, Q.; Yuan, W.; Wang, B.; Zhu, J. Robust, Fire-Safe, Monomer-Recovery, Highly Malleable Thermosets from Renewable Bioresources. *Macromolecules* **2018**, *51*, 8001−8012.
(12) Mondal, S.; Lessard, J. J.; Meena, C. L.; Sanjayan, G. J.; Sumerlin, B. S. Janus Cross-Links in Supramolecular Networks. *J. Am. Chem. Soc.* **2022**, *144*, 845−853.
(13) Mukherjee, S.; Bapat, A. P.; Hill, M. R.; Sumerlin, B. S. Oximes as Reversible Links in Polymer Chemistry: Dynamic Macromolecular Stars. *Polym. Chem.* **2014**, *5*, 6923−6931.
(14) Elling, B. R.; Dichtel, W. R. Reprocessable Cross-Linked Polymer Networks: Are Associative Exchange Mechanisms Desirable? *ACS Cent. Sci.* **2020**, *6*, 1488−1496.
(15) Sun, H.; Kabb, C. P.; Sumerlin, B. S. Thermally-labile Segmented Hyperbranched Copolymers: Using Reversible-Covalent Chemistry to Investigate the Mechanism of Self-Condensing Vinyl Copolymerization. *Chem. Sci.* **2014**, *5*, 4646−4655.
(16) Kabb, C. P.; O'Bryan, C. S.; Deng, C. C.; Angelini, T. E.; Sumerlin, B. S. Photoreversible Covalent Hydrogels for Soft-Matter Additive Manufacturing. *ACS Appl. Mater. Interfaces* **2018**, *10*, 16793−16801.
(17) Han, J.; Liu, T.; Hao, C.; Zhang, S.; Guo, B.; Zhang, J. A Catalyst-Free Epoxy Vitrimer System Based on Multifunctional Hyperbranched Polymer. *Macromolecules* **2018**, *51*, 6789−6799.
(18) Lessard, J. J.; Garcia, L. F.; Easterling, C. P.; Sims, M. B.; Bentz, K. C.; Arencibia, S.; Savin, D. A.; Sumerlin, B. S. Catalyst-Free Vitrimers from Vinyl Polymers. *Macromolecules* **2019**, *52*, 2105−2111.
(19) Osthoff, R. C.; Bueche, A. M.; Grubb, W. T. Chemical Stress-Relaxtion of Polydimethylsiloxane Elastomers. *J. Am. Chem. Soc.* **1954**, *76*, 4659−4663.
(20) Scott, T. F.; Schneider, A. D.; Cook, W. D.; Bowman, C. N. Photoinduced Plasticity in Cross-Linked Polymers. *Science* **2005**, *308*, 1615−1617.
(21) Scott, T. F.; Draughon, R. B.; Bowman, C. N. Actuation in Crosslinked Polymers via Photoinduced Stress Relaxation. *Adv. Mater.* **2006**, *18*, 2128−2132.
(22) Kloxin, C. J.; Scott, F. T.; Bowman, N. C. Stress Relaxation via Addition Fragmentation Chain Transfer in a Thiol-Ene Photopolymerization. *Macromolecules* **2009**, *42*, 2551−2556.
(23) Montarnal, D.; Capelot, M.; Tournilhac, F.; Leibler, L. Silica-like Malleable Materials from Permanent Organic Networks. *Science* **2011**, *334*, 965−968.
(24) Capelot, M.; Montarnal, D.; Tournilhac, F.; Leibler, L. Metal-Catalyzed Transesterification for Healing and Assembling of Thermosets. *J. Am. Chem. Soc.* **2012**, *134*, 7664−7667.
(25) Guerre, M.; Taplan, C.; Winne, J. M.; Du Prez, F. E. Vitrimers: Directing Chemical Reactivity to Control Material Properties. *Chem. Sci.* **2020**, *11*, 4855−4870.
(26) El-Zaatari, B. M.; Ishibashi, J. S. A.; Kalow, J. A. Cross-linker Control of Vitrimer Flow. *Polym. Chem.* **2020**, *11*, 5339−5345.
(27) Ricarte, R. G.; Shanbhag, S. Unentangled Vitrimer Melts: Interplay between Chain Relaxation and Cross-Link Exchange Controls Linear Rheology. *Macromolecules* **2021**, *54*, 3304−3320.
(28) Winne, J. M.; Leibler, L.; Du Prez, F. E. Dynamic Covalent Chemistry in Polymer Networks: A Mechanistic Perspective. *Polym. Chem.* **2019**, *10*, 6091−6108.
(29) Debnath, S.; Kaushal, S.; Ojha, U. Catalyst-Free Partially Bio-Based Polyester Vitrimers. *ACS Appl. Polym. Mater.* **2020**, *2*, 1006−1013.
(30) Denissen, W.; Rivero, G.; Nicolaÿ, R.; Leibler, L.; Winne, J. M.; Du Prez, F. E. Vinylogous Urethane Vitrimers. *Adv. Funct. Mater.* **2015**, *25*, 2451−2457.
(31) Jiang, L.; Liu, Z.; Lei, Y.; Yuan, Y.; Wu, B.; Lei, J. Sustainable Thermosetting Polyurea Vitrimers Based on a Catalyst-Free Process with Reprocessability, Permanent Shape Reconfiguration and Self-Healing Performance. *ACS Appl. Polym. Mater.* **2019**, *1*, 3261−3268.
(32) Ishibashi, J. S. A.; Kalow, J. A. Vitrimeric Silicone Elastomers Enabled by Dynamic Meldrum's Acid-Derived Cross-Links. *ACS Macro Lett.* **2018**, *7*, 482−486.
(33) Zhou, Z.; Su, X.; Liu, J.; Liu, R. Synthesis of Vanillin-Based Polyimine Vitrimers with Excellent Reprocessability, Fast Chemical Degradability, and Adhesion. *ACS Appl. Polym. Mater.* **2020**, *2*, 5716−5725.
(34) Cash, J. J.; Kubo, T.; Bapat, A. P.; Sumerlin, B. S. Room-Temperature Self-Healing Polymers Based on Dynamic-Covalent Boronic Esters. *Macromolecules* **2015**, *48*, 2098−2106.
(35) Bapat, A. P.; Sumerlin, B. S.; Sutti, A. Bulk Network Polymers with Dynamic B − O Bonds: Healable and Reprocessable Materials. *Mater. Horiz.* **2020**, *7*, 694−714.
(36) Zych, A.; Tellers, J.; Bertolacci, L.; Ceseracciu, L.; Marini, L.; Mancini, G.; Athanassiou, A. Biobased, Biodegradable, Self-Healing Boronic Ester Vitrimers from Epoxidized Soybean Oil Acrylate. *ACS Appl. Polym. Mater.* **2021**, *3*, 1135−1144.
(37) Liu, M.; Zhong, J.; Li, Z.; Rong, J.; Yang, K.; Zhou, J.; Shen, L.; Gao, F.; Huang, X.; He, H. A High Stiffness and Self-Healable Polyurethane Based on Disulfide Bonds and Hydrogen Bonding. *Eur. Polym. J.* **2020**, *124*, No. 109475.
(38) Fortman, D. J.; Snyder, R. L.; Sheppard, D. T.; Dichtel, W. R. Rapidly Reprocessable Cross-Linked Polyhydroxyurethanes Based on Disulfide Exchange. *ACS Macro Lett.* **2018**, *7*, 1226−1231.
(39) Chen, J. H.; Hu, D. D.; Li, Y. D.; Zhu, J.; Du, A. K.; Zeng, J. B. Castor Oil-Based High Performance and Reprocessable Poly-(Urethane Urea) Network. *Polym. Test.* **2018**, *70*, 174−179.
(40) Bañales, A. J. M.; Larsen, M. B. Thermal Guanidine Metathesis for Covalent Adaptable Networks. *ACS Macro Lett.* **2020**, *9*, 937−943.
(41) Fortman, D. J.; Brutman, J. P.; Cramer, C. J.; Hillmyer, M. A.; Dichtel, W. R. Mechanically Activated, Catalyst-Free Polyhydroxyurethane Vitrimers. *J. Am. Chem. Soc.* **2015**, *137*, 14019−14022.
(42) Wang, C.; Goldman, T. M.; Worrell, B. T.; McBride, M. K.; Alim, M. D.; Bowman, C. N. Recyclable and Repolymerizable Thiol-X Photopolymers. *Mater. Horiz.* **2018**, *5*, 1042−1046.
(43) Wang, Y.; Pan, Y.; Zheng, Z.; Ding, X. Reconfigurable and Reprocessable Thermoset Shape Memory Polymer with Synergetic Triple Dynamic Covalent Bonds. *Macromol. Rapid Commun.* **2018**, *39*, No. 1800128.
(44) Jiang, Z.; Bhaskaran, A.; Aitken, H. M.; Shackleford, I. C. G.; Connal, L. A. Using Synergistic Multiple Dynamic Bonds to

https://doi.org/10.1021/acs.macromol.2c01909
Macromolecules 2022, 55, 10052−10061

Construct Polymers with Engineered Properties. *Macromol. Rapid Commun.* **2019**, *40*, No. 1900038.
(45) Hammer, L.; Van Zee, N. J.; Nicolaÿ, R. Dually Crosslinked Polymer Networks Incorporating Dynamic Covalent Bonds. *Polymers* **2021**, *13*, No. 396.
(46) Yu, S.; Zhang, G.; Wu, S.; Tang, Z.; Guo, B.; Zhang, L. Effects of Dynamic Covalent Bond Multiplicity on the Performance of Vitrimeric Elastomers. *J. Mater. Chem. A* **2020**, *8*, 20503−20512.
(47) Capelot, M.; Unterlass, M. M.; Tournilhac, F.; Leibler, L. Catalytic Control of the Vitrimer Glass Transition. *ACS Macro Lett.* **2012**, *1*, 789−792.
(48) Self, J. L.; Dolinski, N. D.; Zayas, M. S.; De Alaniz, J. R.; Bates, C. M. Brønsted-Acid-Catalyzed Exchange in Polyester Dynamic Covalent Networks. *ACS Macro Lett.* **2018**, *7*, 817−821.
(49) Delahaye, M.; Winne, J. M.; Du Prez, F. E. Internal Catalysis in Covalent Adaptable Networks: Phthalate Monoester Transesterification as a Versatile Dynamic Cross-Linking Chemistry. *J. Am. Chem. Soc.* **2019**, *141*, 15277−15287.
(50) Moazzen, K.; Rossegger, E.; Alabiso, W.; Shaukat, U.; Schlögl, S. Role of Organic Phosphates and Phosphonates in Catalyzing Dynamic Exchange Reactions in Thiol-Click Vitrimers. *Macromol. Chem. Phys.* **2021**, *222*, No. 2100072.
(51) Altuna, F. I.; Hoppe, C. E.; Williams, R. J. J. Epoxy Vitrimers with a Covalently Bonded Tertiary Amine as Catalyst of the Transesterification Reaction. *Eur. Polym. J.* **2019**, *113*, 297−304.
(52) Zhang, H.; Majumdar, S.; Van Benthem, R. A. T. M.; Sijbesma, R. P.; Heuts, J. P. A. Intramolecularly Catalyzed Dynamic Polyester Networks Using Neighboring Carboxylic and Sulfonic Acid Groups. *ACS Macro Lett.* **2020**, *9*, 272−277.
(53) Kang, B.; Kalow, J. A. Internal and External Catalysis in Boronic Ester Networks. *ACS Macro Lett.* **2022**, *11*, 391−401.
(54) Barsoum, D. N.; Kirinda, V. C.; Kang, B.; Kalow, J. A. Remote-Controlled Exchange Rates by Photoswitchable Internal Catalysis of Dynamic Covalent Bonds. *J. Am. Chem. Soc.* **2022**, *144*, 10168−10173.
(55) Delahaye, M.; Tanini, F.; Holloway, J. O.; Winne, J. M.; Du Prez, F. E. Double Neighbouring Group Participation for Ultrafast Exchange in Phthalate Monoester Networks. *Polym. Chem.* **2020**, *11*, 5207−5215.
(56) Nishimura, Y.; Chung, J.; Muradyan, H.; Guan, Z. Silyl Ether as a Robust and Thermally Stable Dynamic Covalent Motif for Malleable Polymer Design. *J. Am. Chem. Soc.* **2017**, *139*, 14881−14884.
(57) Cromwell, O. R.; Chung, J.; Guan, Z. Malleable and Self-Healing Covalent Polymer Networks through Tunable Dynamic Boronic Ester Bonds. *J. Am. Chem. Soc.* **2015**, *137*, 6492−6495.
(58) Spiesschaert, Y.; Taplan, C.; Stricker, L.; Guerre, M.; Winne, J. M.; Du Prez, F. E. Influence of the Polymer Matrix on the Viscoelastic Behaviour of Vitrimers. *Polym. Chem.* **2020**, *11*, 5377−5385.
(59) Hajj, R.; Duval, A.; Dhers, S.; Avérous, L. Network Design to Control Polyimine Vitrimer Properties: Physical Versus Chemical Approach. *Macromolecules* **2020**, *53*, 3796−3805.
(60) Cash, J. J.; Kubo, T.; Dobbins, D. J.; Sumerlin, B. S. Maximizing the Symbiosis of Static and Dynamic Bonds in Self-Healing Boronic Ester Networks. *Polym. Chem.* **2018**, *9*, 2011−2020.
(61) Lee, J.; Jing, B. B.; Porath, L. E.; Sottos, N. R.; Evans, C. M. Shock Wave Energy Dissipation in Catalyst-Free Poly(Dimethylsiloxane) Vitrimers. *Macromolecules* **2020**, *53*, 4741−4747.
(62) Schoustra, S. K.; Groeneveld, T.; Smulders, M. M. J. The Effect of Polarity on the Molecular Exchange Dynamics in Imine-Based Covalent Adaptable Networks. *Polym. Chem.* **2021**, *12*, 1635−1642.
(63) Guerre, M.; Taplan, C.; Nicolaÿ, R.; Winne, J. M.; Du Prez, F. E. Fluorinated Vitrimer Elastomers with a Dual Temperature Response. *J. Am. Chem. Soc.* **2018**, *140*, 13272−13284.
(64) Self, J. L.; Sample, C. S.; Levi, A. E.; Li, K.; Xie, R.; De Alaniz, J. R.; Bates, C. M. Dynamic Bottlebrush Polymer Networks: Self-Healing in Super-Soft Materials. *J. Am. Chem. Soc.* **2020**, *142*, 7567−7573.
(65) Ricarte, R. G.; Tournilhac, F.; Leibler, L. Phase Separation and Self-Assembly in Vitrimers: Hierarchical Morphology of Molten and Semicrystalline Polyethylene/Dioxaborolane Maleimide Systems. *Macromolecules* **2019**, *52*, 432−443.
(66) Lessard, J. J.; Scheutz, G. M.; Hughes, R. W.; Sumerlin, B. S. Polystyrene-Based Vitrimers: Inexpensive and Recyclable Thermosets. *ACS Appl. Polym. Mater.* **2020**, *2*, 3044−3048.
(67) Lessard, J. J.; Scheutz, G. M.; Sung, S. H.; Lantz, K. A.; Epps, T. H.; Sumerlin, B. S. Block Copolymer Vitrimers. *J. Am. Chem. Soc.* **2020**, *142*, 283−289.
(68) Ishibashi, J. S. A.; Pierce, I. C.; Chang, A. B.; Zografos, A.; Elzaatari, B. M.; Fang, Y.; Weigand, S. J.; Bates, F. S.; Kalow, J. A. Mechanical and Structural Consequences of Associative Dynamic Cross-Linking in Acrylic Diblock Copolymers. *Macromolecules* **2021**, *54*, 3972−3986.
(69) Hill, M. R.; Carmean, R. N.; Sumerlin, B. S. Expanding the Scope of RAFT Polymerization: Recent Advances and New Horizons. *Macromolecules* **2015**, *48*, 5459−5469.
(70) Perrier, S. 50th Anniversary Perspective: RAFT Polymerization - A User Guide. *Macromolecules* **2017**, *50*, 7433−7447.
(71) Wang, S.; Li, L.; Liu, Q.; Urban, M. W. Self-Healable Acrylic-Based Covalently Adaptable Networks. *Macromolecules* **2022**, *55*, 4703−4709.
(72) Sajjad, H.; Tolman, W. B.; Reineke, T. M. Block Copolymer Pressure-Sensitive Adhesives Derived from Fatty Acids and Triacetic Acid Lactone. *ACS Appl. Polym. Mater.* **2020**, *2*, 2719−2728.
(73) Peticolas, W. L. Molecular Weight Distribution of Linear Polymers from Stress Relaxation in Polymer Melts. *J. Chem. Phys.* **1963**, *39*, 3392−3400.
(74) Gentekos, D. T.; Sifri, R. J.; Fors, B. P. Controlling Polymer Properties through the Shape of the Molecular-Weight Distribution. *Nat. Rev. Mater.* **2019**, *4*, 761−774.
(75) Gentekos, D. T.; Jia, J.; Tirado, E. S.; Barteau, K. P.; Smilgies, D. M.; Distasio, R. A.; Fors, B. P. Exploiting Molecular Weight Distribution Shape to Tune Domain Spacing in Block Copolymer Thin Films. *J. Am. Chem. Soc.* **2018**, *140*, 4639−4648.
(76) Whitfield, R.; Truong, N. P.; Anastasaki, A. Precise Control of Both Dispersity and Molecular Weight Distribution Shape by Polymer Blending. *Angew. Chem., Int. Ed.* **2021**, *60*, 19383−19388.
(77) Shimizu, T.; Truong, N. P.; Whitfield, R.; Anastasaki, A. Tuning Ligand Concentration in Cu(0)-RDRP: A Simple Approach to Control Polymer Dispersity. *ACS Polym. Au* **2021**, *1*, 187−195.
(78) Leibler, L.; Rubinstein, M.; Colby, R. H. Dynamics of reversible networks. *Macromolecules* **1991**, *24*, 4701−4707.
(79) Leibler, L.; Rubinstein, M.; Colby, R. H. Dynamics of telechelic ionomers. Can polymers diffuse large distances without relaxing stress? *J. Phys. II* **1993**, *3*, 1581−1590.
(80) Rubinstein, M.; Semenov, A. N. Thermoreversible gelation in solutions of associating polymers. 2. Linear dynamics. *Macromolecules* **1998**, *31*, 1386−1397.
(81) Rubinstein, M.; Semenov, A. N. Dynamics of entangled solutions of associating polymers. *Macromolecules* **2001**, *34*, 1058−1068.
(82) Wu, S.; Chen, Q. Advances and New Opportunities in the Rheology of Physically and Chemically Reversible Polymers. *Macromolecules* **2022**, *55*, 697−714.
(83) Cooper, C. B.; Kang, J.; Yin, Y.; Yu, Z.; Wu, H. C.; Nikzad, S.; Ochiai, Y.; Yan, H.; Cai, W.; Bao, Z. Multivalent Assembly of Flexible Polymer Chains into Supramolecular Nanofibers. *J. Am. Chem. Soc.* **2020**, *142*, 16814−16824.
(84) Rouse, P. E., Jr A theory of the linear viscoelastic properties of dilute solutions of coiling polymers. *J. Chem. Phys.* **1953**, *21*, 1272−1280.
(85) Chen, Q.; Tudryn, G. J.; Colby, R. H. Ionomer dynamics and the sticky Rouse model. *J. Rheol.* **2013**, *57*, 1441−1462.
(86) Jiang, N.; Zhang, H.; Tang, P.; Yang, Y. Linear viscoelasticity of associative polymers: Sticky Rouse model and the role of bridges. *Macromolecules* **2020**, *53*, 3438−3451.
(87) de Gennes, P. G. Kinetics of diffusion-controlled processes in dense polymer systems. I. Nonentangled regimes. *J. Chem. Phys.* **1982**, *76*, 3316−3321.

https://doi.org/10.1021/acs.macromol.2c01909
Macromolecules 2022, 55, 10052−10061

(88) Rubinstein, M.; Helfand, E.; Pearson, D. S. Theory of polydispersity effects of polymer rheology: Binary distribution of molecular weights. *Macromolecules* **1987**, *20*, 822−829.

https://doi.org/10.1021/acs.macromol.2c01909
Macromolecules 2022, 55, 10052−10061